

and/or hydrolysis of phosphazene–thiazyl systems containing three-coordinate sulfur will provide an alternative route to hybrid ring systems containing four-coordinate sulfur. Since there is a variety of ring sizes available for phosphazene–thiazyl rings (six-<sup>3,18</sup> eight-<sup>19,20</sup> and twelve-membered<sup>1</sup> rings are known), this approach offers the possibility of extending the

range of mixed phosphazene–sulfanuric systems to rings larger than six atoms.

**Acknowledgment.** We thank the NSERC (Canada) for financial support.

**Supplementary Material Available:** Listings of anisotropic thermal parameters for non-hydrogen atoms, positional and isotropic thermal parameters for hydrogen atoms, bond lengths and bond angles for phenyl groups, least-squares planes, and observed and calculated structure factors for **4** and **5** (106 pages). Ordering information is given on any current masthead page.

- (18) Pohl, S.; Petersen, O.; Roesky, H. W. *Chem. Ber.* **1977**, *112*, 1545.  
 (19) Appel, R.; Eichenhofer, K. W. *Chem. Ber.* **1971**, *104*, 3859.  
 (20) Burford, N.; Chivers, T.; Richardson, J. F. *Inorg. Chem.*, in press.

Contribution from the Institute of Inorganic Chemistry, University of Frankfurt, Niederurseler Hang, D-6000 Frankfurt (M) 50, FRG, and Fachbereich Chemie, Freie Universität Berlin, FB 21, D-1000 Berlin 33, FRG

## The Isomers F<sub>3</sub>CNC and F<sub>3</sub>CCN: Photoelectron Spectra, Thermal Rearrangement, and Effects of Fluorine Substitution on Parent Molecules C<sub>2</sub>H<sub>3</sub>N<sup>§,1,2</sup>

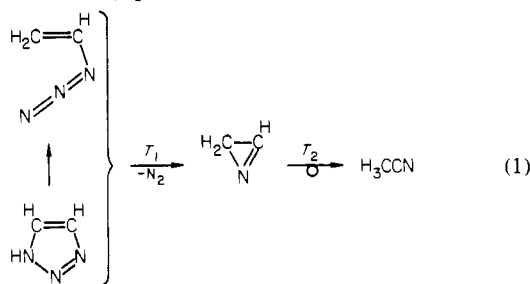
H. BOCK,\*† R. DAMMEL,† and D. LENTZ†

Received March 25, 1983

The thermal rearrangement F<sub>3</sub>CNC → F<sub>3</sub>CCN has been monitored by photoelectron (PE) spectroscopy in a gaseous flow system. In contrast to the rather limited stability of liquid F<sub>3</sub>CNC, the isomerization in the gas phase requires temperatures above 750 K, suggesting a considerable kinetic barrier. MNDO calculations for various compounds C<sub>2</sub>F<sub>3</sub>N support the assignment of the He I and the He II PE spectra recorded for F<sub>3</sub>CNC and F<sub>3</sub>CCN, allow an estimate of the relative thermodynamical stabilities of the C<sub>2</sub>F<sub>3</sub>N isomers and, by comparison with the parent species C<sub>2</sub>H<sub>3</sub>N, provide insight into the effects of fluorine substitution C<sub>2</sub>H<sub>3</sub>N ↔ C<sub>2</sub>F<sub>3</sub>N within these six-atom molecules and their radical cations.

### Introduction

The relative stabilities and interconversions of various "valence normal" C<sub>2</sub>H<sub>3</sub>N isomers have recently been the subject of a number of experimental<sup>3</sup> and theoretical<sup>3–5</sup> investigations. For example, the thermal decompositions of vinyl azide and its isomer, 1,2,3(1*H*)-triazole, monitored by PE spectroscopy, yield 2*H*-azirine as a trappable intermediate which only at higher temperature rearranges to the most stable isomer acetonitrile<sup>3</sup> (eq 1).

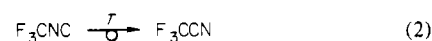


Accompanying MNDO<sup>3</sup> as well as ab initio calculations<sup>4,5</sup> fully reproduce the experimental observations and allow estimates on the unexpectedly high N<sub>2</sub> extrusion and isomerization barriers within the six-atom isomer ensemble C<sub>2</sub>H<sub>3</sub>N.

Little information, however, is available on the C<sub>2</sub>F<sub>3</sub>N ensemble of compounds, where the interest has focused on the two known isomers, trifluoroacetonitrile, F<sub>3</sub>CC≡N, and trifluoromethyl isocyanide, F<sub>3</sub>CN≡C, and their isomerization.<sup>6</sup> Whereas trifluoroacetonitrile, as acetonitrile itself, is a perfectly stable compound, trifluoromethyl isocyanide exhibits remarkably reduced stability compared to methyl isocyanide, especially in the condensed phase (see Experimental Section). This is in accordance with the lack of data on isocyanides with

strong acceptor substituents, especially perfluoroalkyl-substituted ones.

In the following, a combination of photoelectron (PE) spectroscopy and semiempirical MNDO calculations is used to investigate the effects of fluorine substitution on H<sub>3</sub>CN≡C and H<sub>3</sub>CC≡N and to establish the isomer stability sequences for the neutral and positively charged ensembles C<sub>2</sub>X<sub>3</sub>N with X = H and F. With trifluoromethyl isocyanide predicted to be thermodynamically 130 kJ/mol less stable than trifluoroacetonitrile, the thermal rearrangement



is investigated in a gaseous flow system with use of PE spectroscopic real-time analysis.<sup>3</sup>

### Experimental Section

Trifluoromethyl isocyanide has previously been prepared via the reaction of F<sub>3</sub>CNHCF<sub>2</sub>Br with magnesium,<sup>7</sup> pyrolysis of the imino-

- (1) Photoelectron Spectra and Molecular Properties. 107. Part 106: Bürger, M.; Pawelke, G.; Dammel, R.; Bock, H. *J. Fluorine Chem.* **1982**, *19*, 565.
- (2) Part of the Ph.D. thesis of R. Dammel, University of Frankfurt, 1983.
- (3) The review on PE spectroscopic gas analysis by Bock and Solouki (Bock, H.; Solouki, B. *Angew. Chem.* **1981**, *93*, 435; *Angew. Chem., Int. Ed. Engl.* **1981**, *20*, 437) includes among the various examples for its application a preliminary report on the pyrolysis of vinyl azide and the accompanying hypersurface calculations.
- (4) Bock, H.; Dammel, R.; Aygen, S. *J. Am. Chem. Soc.* **1983**, *105*, 7681. Cf. ref 3 or the summary on semiempirical hypersurface calculations by the Frankfurt PES group by: Bock, H.; Dammel, R.; Roth, B. In "Inorganic Rings and Clusters"; Cowley, A., Ed.; American Chemical Society: Washington, DC, 1983; pp 139–165.
- (5) Ab initio SCF calculations including configuration interaction on the vinyl azide decomposition have been performed by L. L. Lohr, Jr., M. Hanamura, and K. Morukuma: *J. Am. Chem. Soc.* **1983**, *105*, 5541. See also: Torres, M.; Lown, E. M.; Gunning, H. E.; Strausz, O. P. *Pure Appl. Chem.* **1980**, *52*, 1623.
- (6) Moffat, J. B. *Chem. Phys. Lett.* **1978**, *55*, 125.
- (7) Makarov, S. P.; Englin, M. A.; Videiko, A. F.; Nikolaeva, T. V. *Zh. Obshch. Khim.* **1968**, *37*, 2781.

§To the memory of Earl L. Muettterties.

†University of Frankfurt.

‡Freie Universität Berlin.

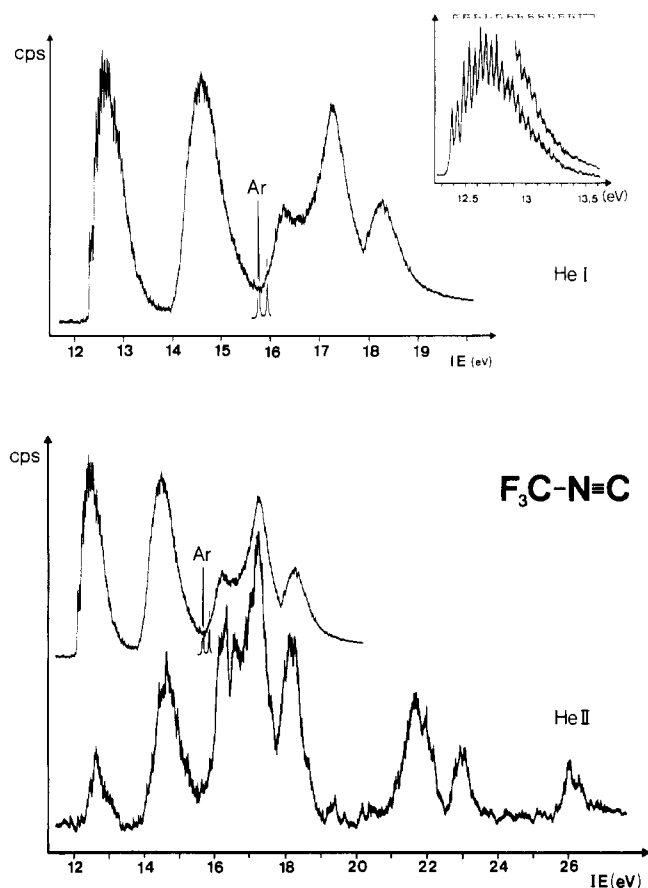
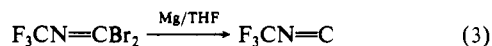


**Figure 1.** He I and He II PE spectra of trifluoromethyl isocyanide,  $F_3CNC$ . The inset shows the vibrational fine structure of the first band. The He I spectrum is displayed again above the He II spectrum reduced to the same scale for better comparison.

substituted phosphoric ester  $F_3CN=CFPF(OEt)_3$ ,<sup>8</sup> or thermal extrusion of carbonyl fluoride from the azabutenoil fluoride  $F_3CN=CFCOF$ .<sup>9</sup> All these reactions suffer from low yields of the isocyanide, which moreover is difficult to separate from byproducts. A recently developed synthesis<sup>10</sup> with excellent yields and facile product workup involves reduction of  $F_3CN=CBr_2$ , described previously as a decomposition product of the aminoborane  $(CF_3)_2NBBR_2$ ,<sup>11</sup> with magnesium in THF



yielding up to 90% of pure trifluoromethyl isocyanide.<sup>10</sup> The compound was characterized by its  $^{19}F$  NMR ( $-80^\circ C$ : single peak at 52 ppm, splitting into three peaks with  $J_{19F-19F} = 15.5$  Hz at  $0^\circ C$ ), IR,<sup>18</sup> and mass spectra<sup>10</sup> and by reaction with a number of metal carbonyls, for one of which,  $Fe_3(CO)_{11}(\mu-CNCF_3)$ , a crystal structure analysis has been performed.<sup>10</sup>

**PE spectra** were recorded on a Leybold-Heraeus UPG 200 spectrometer. Throughout the experiments, resolution was of the order of 18 meV for the He I and about 40 meV for the He II spectra. The  $F_3CNC \rightarrow F_3CCN$  rearrangement has been monitored with a Perkin-Elmer PS 16 spectrometer connected to an externally heated (oven length 30 cm) quartz tube of 1.5 cm diameter.

**MNDO calculations** have been carried out on the University of Frankfurt DEC 1091 computer using the MNDO program kindly provided by M. J. S. Dewar<sup>12</sup> and for the MNDO ASCF calculations a program composed by B. Roth<sup>13</sup> was used. For all compounds, full

**Table I.** Vertical PES Ionization Energies  $IE_n^V$  (eV) for  $F_3CNC$  and  $F_3CCN$  and Their Assignment by MNDO,  $\Delta SCF$  (MNDO), and "Green Function" (GF) Calculations (See Text)

$F_3CNC$			
$IE_n^V$ <sup>a</sup>	assignt	$-\epsilon_f$ <sup>MNDO</sup>	$IE^{\Delta SCF}$
12.60	$n_C(6a_1)$	13.53	12.99
14.60	$\pi_{NC}(5e)$	14.43	13.89
16.28	(4e)	16.48	16.10
(16.7)	$n_{FP}$ {	(1a <sub>2</sub> )	16.68
17.3	(3e)	(3e)	16.93
18.3	(5a <sub>1</sub> )	(5a <sub>1</sub> )	17.00
21.7	(2e)	(2e)	20.49
23.0	$\sigma_{CF}$ {	(4a <sub>1</sub> )	22.16
26.1	(3a <sub>1</sub> )	(3a <sub>1</sub> )	27.48
	$2s_x$ {	(2a <sub>1</sub> )	38.18
	(1e)	(1e)	44.90
	(1a <sub>1</sub> )	(1a <sub>1</sub> )	52.10
$F_3CCN$			
$IE_n^V$ <sup>a</sup>	assignt	$-\epsilon_f$ <sup>MNDO</sup>	$IE^{GF}$ <sup>17</sup>
(14.3)	$\pi_{CN}(5e)$	14.80	14.74
(14.3)	$n_N(6a_1)$	15.11	14.26
(16.3)	(4e)	16.60	17.50
16.56	$n_{FP}$ {	(1a <sub>2</sub> )	16.81
(17.1)	(3e)	(3e)	17.10
18.10	(5a <sub>1</sub> )	(5a <sub>1</sub> )	17.15
21.6	(2e)	(2e)	20.55
22.6	$\sigma_{CF}$ {	(4a <sub>1</sub> )	22.00
25.7	(3a <sub>1</sub> )	(3a <sub>1</sub> )	27.52
	$2s_x$ {	(2a <sub>1</sub> )	38.98
	(1e)	(1e)	44.88
	(1a <sub>1</sub> )	(1a <sub>1</sub> )	52.35

<sup>a</sup> Parentheses denote overlapping bands.

**Table II.** PES Vibrational Frequencies  $\nu^*$  ( $cm^{-1}$ ) for Individual Radical Cation States  $M^+$  Compared to Those ( $\nu$ ,  $cm^{-1}$ ) of the Neutral Molecules (See Text)

$M^+$	$\nu^*$	$\nu$	assignt <sup>10</sup>
$F_3CNC$			
$\tilde{X}(^2A_1)$ {	730	840	$\delta_{CF_3}$
	380	550	$\nu_{NC}$
$F_3CCN$			
$\tilde{X}(^2E)$ {	1000	1227	$\nu_{CF}$
	640	802	$\delta_{CF_3}$
	450	521	$\nu_{CC}$
$\tilde{C}(^2A_2)$	800	802	$\delta_{CF_3}$
$\tilde{D}(^2A_1)$ {	1250	1227	$\nu_{CF}$
	750	802	$\delta_{CF_3}$
	480	521	$\nu_{CC}$

geometry optimization of the neutral ground states was carried out with use of the Davidson-Fletcher-Powell algorithm<sup>14</sup> with standard parameters. The CNC chain in  $F_3CNC$  was found to be linear, in accordance with the analysis of the microwave spectrum.<sup>15</sup>

#### Photoelectron Spectra of the Isomers $F_3CNC$ and $F_3CCN$ and Their Assignment

The He I and He II photoelectron (PE) spectra of  $F_3CNC$  are displayed in Figure 1 and those for  $F_3CCN$  (cf. ref 16,17) in Figure 2. Vertical PES ionization energies and their assignment by quantum-chemical calculations are summarized

- (8) Gontar, A. F.; Til'kunova, N. A.; Bykhovskaja, E. G.; Knunyants, I. L. *Izv. Akad. Nauk SSSR, Ser. Khim.* **1977**, 2379.  
 (9) Banks, R. E.; Haszeldine, R. N.; Stevenson, M. J.; Willoughby, B. G. *J. Chem. Soc. C* **1969**, 2119.  
 (10) Lentz, D. *J. Fluorine Chem.*, in press.  
 (11) Greenwood, N. N.; Hooton, K. A. *J. Chem. Soc. A* **1966**, 751.  
 (12) Dewar, M. J. S.; Thiel, W. *J. Am. Chem. Soc.* **1977**, *99*, 4899, 4907.  
 (13) Roth, B. Ph.D. Thesis, University of Frankfurt, 1983.

- (14) Fletcher, R.; Powell, M. J. D. *Comput. J.* **1963**, *6*, 163. Davidson, W. C. *Ibid.* **1968**, *10*, 406.  
 (15) Oberhammer, H.; Lentz, D., private communications.  
 (16) Cf.: Stafast, H.; Bock, H. In "The Chemistry of Functional Groups"; Patai, S., Ed., Wiley: New York, 1983; pp 137-185. Cf. also: Stafast, H. Ph.D. Thesis, University of Frankfurt, 1974.  
 (17) Åsbrink, L.; Svensson, A.; Niessen, W. v.; Bieri, G. *J. Electron Spectrosc. Relat. Phenom.* **1981**, *24*, 293. Cf. also: Bieri, G.; Heilbronner, E.; Hornung, V.; Kloster-Jensen, E.; Maier, J. P.; Thommen, F.; Niessen, W. v. *Chem. Phys.* **1979**, *36*, 1.  
 (18) Lee, J.; Willoughby, B. G. *Spectrochim. Acta Part A* **1977**, *33A*, 395 and references cited therein.

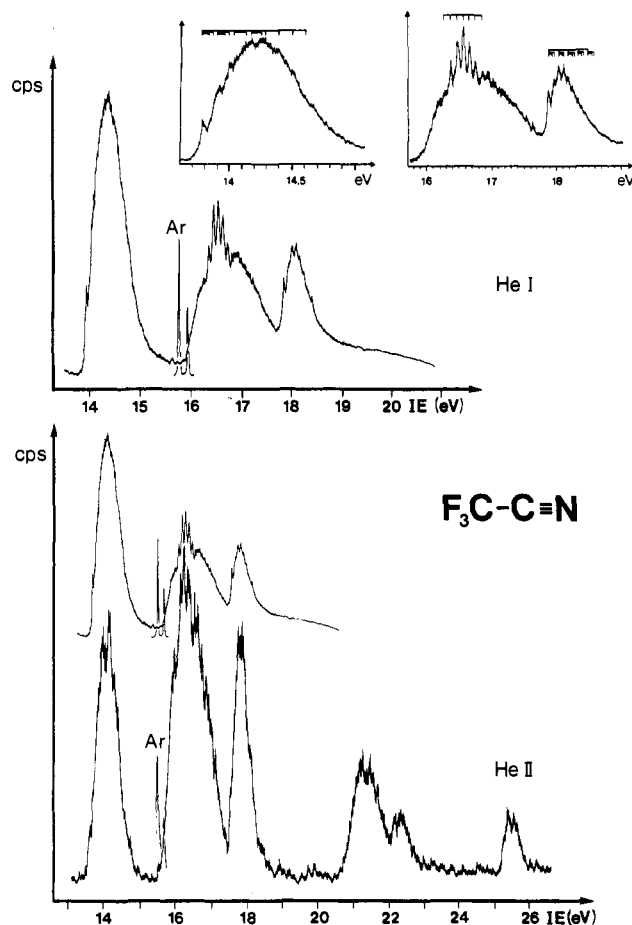


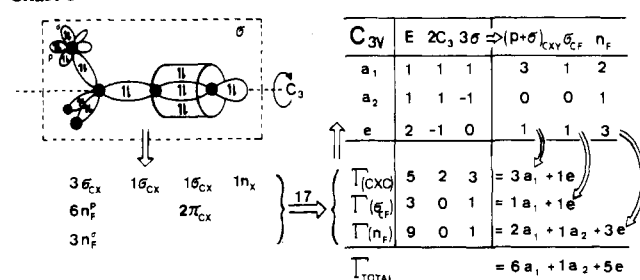
**Figure 2.** He I and He II PE spectra of trifluoroacetonitrile, F<sub>3</sub>CCN. Insets show details of the first band, and the fluorine lone-pair region (16–19 eV). The He I spectrum is displayed again above the He II spectrum reduced to the same scale for better comparison.

in Table I, and the PES vibrational frequencies for individual radical cation states are compared to those for the neutral molecules in Table II.

Obviously, the He I PE spectra of the two C<sub>2</sub>F<sub>3</sub>N isomers (Figures 1 and 2) differ considerably in both band positions and shapes. For example, the ionization pattern of F<sub>3</sub>CNC consists of four band systems, whereas only three are observed for F<sub>3</sub>CCN. As a special feature, the first PE band of F<sub>3</sub>CNC exhibits an extensive vibrational fine structure (Figure 1 and Table II). Its intuitive assignment to the ionization of the isocyanide carbon lone pair n<sub>c</sub> would be in accord with the 1.8-eV shift of the first PE band to higher energy for F<sub>3</sub>CCN (Figure 2 and Table II), where the nitrogen lone pair n<sub>N</sub> ionization due to the increased effective nuclear charge of N relative to that of C is expected to be part of the 14.3-eV band system.

In order to avoid a "black box" assignment for the non PE spectroscopist, the simplified "Linear Combination of Bond Orbitals" approach (cf., e.g., ref 16, 19–21) facilitates the rationalization of ionization patterns (Table I). When the valence electrons of the C<sub>2</sub>F<sub>3</sub>N isomers are counted, 34/2 = 17 electron pairs result. Their distribution over the F<sub>3</sub>CNC and F<sub>3</sub>CCN skeletons, both of C<sub>3v</sub> symmetry, and—after ejection of one electron—the distribution of the positive holes in the corresponding radical cation states can be classified with

Chart I



respect to predominant contributions and their (irreducible) symmetry as shown in Chart I.

Altogether 12 ionizations are expected, of which 5 are doubly degenerate (e), leading to the radical cation states of the symmetry and predominant contribution specified in Chart I. Their sequence as suggested by MNDO calculations<sup>12</sup> applying Koopmans' theorem,  $IE_n^v = -\epsilon_j^{MNDO}$ , is presented in Table I.

For F<sub>3</sub>CNC, the first two ionizations at 12.60 and 14.60 eV correspond to the ejection of carbon lone pair (n<sub>c</sub>) and π<sub>CN</sub> electrons, leading to the radical cation ground state  $\tilde{X}(^2A_1)$  and its first excited state  $\tilde{A}(^2E)$ . The broad band system between 16 and 18 eV comprises the n<sub>F</sub> lone-pair ionizations to the corresponding M<sup>+</sup> states  $\tilde{B}-\tilde{E}$  (denoted  $^2A_2$ ,  $2x^2E$ , and  $^2A_1$ ). In the He II region three more bands are observed (Figure 1), of which the two at 21.7 and 23.0 eV are assigned to M<sup>+</sup> states with predominant σ<sub>CF</sub> contribution, and the one at 26.1 eV is assigned to a 2s<sub>C</sub>-type electron ejection. The other three valence electron ionizations are predicted by the MNDO calculations to be found outside the measurement region.

For the isomer F<sub>3</sub>CCN, the He I and He II PE spectra (Figure 2) exhibit considerably different low-energy ionization patterns: according to the MNDO predictions (Table I), the band of double intensity with a maximum at 14.3 eV should comprise both the π<sub>CN</sub> and n<sub>N</sub> ionizations, with the radical cation ground state  $\tilde{X}(^2E)$ —in contrast to the case for F<sub>3</sub>CNC—now of predominant π<sub>CN</sub> character. The sequence of higher M<sup>+</sup> states is predicted to closely resemble that of the isomer F<sub>3</sub>CNC (Table I), as can be convincingly substantiated by comparison of the two He II PE spectra above 18 eV (Figures 1 and 2).

The above assignment on the basis of semiempirical MNDO calculations applying Koopmans' theorem leads to the following linear regressions for the He I PES region (Table I):

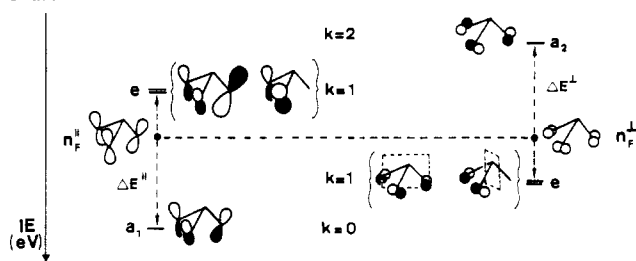
$$\begin{aligned} \text{F}_3\text{CNC: } IE_n^v &= -4.1 + 1.27(-\epsilon_j^{MNDO}); \text{ SE} = 0.5 \text{ eV} \\ \text{F}_3\text{CCN: } IE_n^v &= -4.9 + 1.29(-\epsilon_j^{MNDO}); \text{ SE} = 0.4 \text{ eV} \end{aligned} \quad (4)$$

Although the resulting standard errors SE are slightly outside satisfactory limits as usually achieved by MNDO assignments of PE spectra,<sup>22</sup> they still support the applicability of this semiempirical procedure also to highly fluorine-substituted molecules of medium size.<sup>23</sup> Nevertheless, caution is advised especially in regions of densely packed radical cation states such as the fluorine lone-pair ionization region between 16.5 and 17.2 eV (Table I). In addition, within the Koopmans approximation, both the changes in the wave function for M<sup>+</sup> and the differences in electron correlation between M and M<sup>+</sup> are neglected.<sup>24</sup> The first shortcoming can be largely accounted for by performing independent calculations for the

(19) Cf., e.g.: Bock, H. *Pure Appl. Chem.* **1975**, *44*, 342 and references given.  
 (20) Cf., e.g.: Wittel, K.; Bock, H. In "The Chemistry of Functional Groups"; Patai, S., Ed.; Wiley: New York, 1983; pp 1499–1603 and literature cited therein.  
 (21) Cf., e.g.: Bock, H.; Ramsey, B. *Angew. Chem.* **1973**, *85*, 773; *Angew. Chem., Int. Ed. Engl.* **1973**, *12*, 734 and literature cited therein.

(22) Cf., e.g.: Bock, H.; Dammel, R.; Roth, B. In "Inorganic Rings and Clusters"; American Chemical Society: Washington, DC, 1983; pp 139–165.  
 (23) Cf., e.g.: Dewar, M. J. S.; Rzepa, H. R. *J. Am. Chem. Soc.* **1978**, *100*, 58 and references given therein.  
 (24) Cf., e.g.: Kutzelnigg, W. "Einführung in die Theoretische Chemie"; Verlag Chemie: Weinheim, Germany, 1978; Vol. 2, pp 249 ff, 552 ff.

Chart II



ground state of  $M$  and the different states of  $M^+$  and subtracting their total energies. Within this approximation the  $\Delta E^{\text{SCF}}$  values for  $F_3CNC$  (Table I) show no changes in the  $M^+$  state sequence predicted by the MNDO eigenvalues. The electron correlation is more difficult to incorporate,<sup>24</sup> and the "Green function" calculation results quoted for  $F_3CCN$ <sup>17</sup> indeed show considerably deviations (Table I). Therefore, additional support for the assignment of the PES ionization patterns based on spectroscopic features and, above all, on comparison of equivalent radical cation states of chemically related molecules (cf. e.g., ref 16, 19–21,<sup>25</sup>) shall be presented.

To start with, the MNDO-predicted  $M^+$  state sequence for  $F_3CCN$ ,  $\tilde{X}(^2E)$  below  $\tilde{A}(^2A_1)$ , is in accord with other experimental observations. Band intensities in He I and He II PE spectra usually differ due to different ionization cross sections,<sup>26</sup> and although any predictions are by no means straightforward, often an increase in  $\pi$ -type ionization intensities—including  $\pi_{CN}$  ionizations<sup>27</sup>—relative to those of  $\sigma$  character has been observed. Thus, the tremendous He I/He II intensity reduction of the first PE band of  $F_3CNC$  (Figure 1) unequivocally confirms the assignment to the  $\sigma$ -type carbon lone-pair ionization. For  $F_3CCN$ , the intensity of the first band system is relatively decreased, the center being slightly shifted to lower energy and the vibrational fine structure increased (Figure 2)—as one would expect if the  $\pi_{CN}$  ionization were lower than that of the  $\sigma$ -type  $n_N$  lone pair.

For the differing MNDO vs. GF assignments in the  $n_F^p$  lone pair ionization region (Table I), comparisons with other small molecules containing  $F_3X$  subunits of  $C_{3v}$  symmetry shall be quoted. From qualitative arguments based on symmetry and on the number of nodal planes in the LCO combinations (Chart I) the order of ionization energies of the two formally independent sets of the vertical ( $n_F^p$ : e above  $a_1$ ) and horizontal ( $n_F^h$ : e below  $a_2$ ) fluorine lone pairs given by Chart II is expected.<sup>19</sup> If other interactions are neglected, the resulting  $n_F$  radical cation state sequence depends on the relative magnitudes of the  $n_F$  splittings,  $\Delta E^p$  vs.  $\Delta E^h$ : for  $\Delta E^p \approx \Delta E^h$  an ionization pattern  $a_2 < e < e < a_1$  is predicted as observed for  $HCF_3$ <sup>28,29</sup> or, more clearly, in the series of  $F_3P$ ,  $F_2P \cdot BH_3$ ,  $F_3PS$ , and  $F_3PO$ ,<sup>19</sup> whereas for  $\Delta E^p > \Delta E^h$  one expects an ordering  $e < a_2 < e < a_1$  as assigned for the PE spectra of  $F_3CNC$  and  $F_3CNC$  (Table I).

A molecular radical cation state correlation diagram (Figure 3) for  $F_3CNC$  and  $F_3CCN$  together with the hydrogen-substituted parent molecules  $C_2H_3N$ <sup>16,30</sup> and with the isoelectronic 3,3,3-trifluoropropyne ( $CH \hat{=} N$ ) lends further credence to

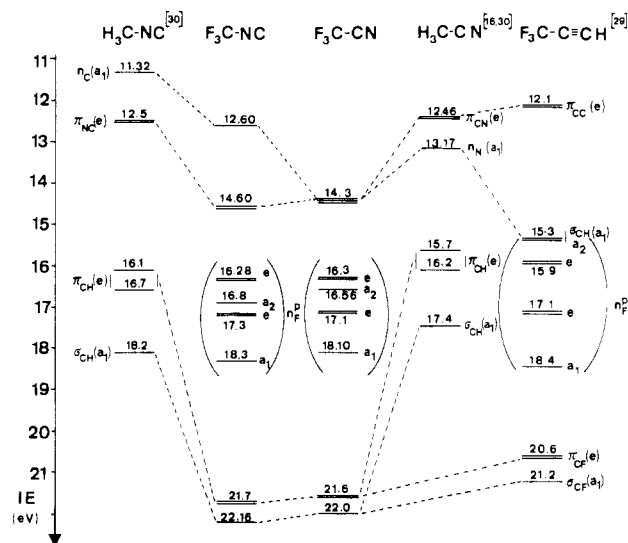
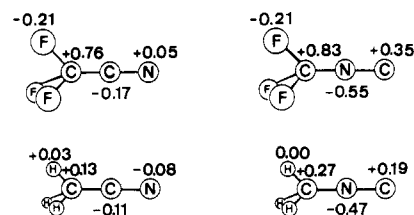


Figure 3.  $M^+$  state correlation diagram for the isomers  $F_3CNC$  and  $F_3CCN$  as well as  $H_3CNC$  and  $H_3CCN$ , supplemented by the PES ionization pattern of the isoelectronic  $F_3CC \equiv CH$ .

Chart III



the PE spectroscopic assignment proposed. Among the many features of this diagram, the following are emphasized: also for the parent compounds  $H_3CNC$  and  $H_3CCN$ , the first two ionizations change their sequence from  $n_C(a_1) > \pi_{NC}(e)$  to  $\pi_{CN}(e) > n_N(a_1)$ .<sup>30</sup> On isoelectronic substitution  $N \rightarrow CH$  in  $F_3CC \equiv N$  to  $F_3CC \equiv CH$ , the  $\pi_{CN}(e)$  ionization is raised to 12.1 eV, whereas the lone pair  $n_N$  is transformed into a  $\sigma_{CH}$  bond, which because of the additional hydrogen potential is ionized only at 15.3 eV. The  $C_2H_3N^+$  states with predominant  $\sigma_{CH}$  contribution are shifted on fluorine substitution due to the increased effective nuclear charge to the 21–22-eV region, with an analogous effect also being observed for  $F_3CC \equiv CH$ . The corresponding  $M^+$  states of predominant  $\sigma_{CF}$  character and of e and  $a_1$  symmetry show some mixing with the  $n_F^+$  states of the same symmetry. Nevertheless, the fluorine lone-pair ionization patterns are found consistently in the 16–18-eV region, as in many other molecules with  $F_3X$  subunits of (local)  $C_{3v}$  symmetry.

In return, the  $M^+$  state correlation diagram (Figure 3), based on PES assignments, further supports the reliability of the MNDO results (cf. (4) and Table I). Therefore, in addition MNDO charge distributions<sup>12,23</sup> for trifluoromethyl isocyanide and trifluoroacetonitrile are presented, which in comparison with those of the unsubstituted parent compounds show several intriguing features (Chart III). As is obvious, F substitution enhances the positive charge on the carbon atom of the  $CF_3$  group quite strongly and withdraws electron density from the terminal C or N atom, so that the central atom (C or N) becomes more negative. Within the concept of  $\sigma$ -accepting/ $\pi$ -back-donating properties of fluorine substituents<sup>31</sup> these changes in the MNDO charges (Chart III) can be rationalized by strong withdrawal of charge from the  $\sigma$  skeleton and an accompanying polarization of the  $\pi$  electron cloud.

(25) Cf., e.g.: Bock, H. *Angew. Chem.* 1977, 89, 631; *Angew. Chem., Int. Ed. Engl.* 1977, 16, 613 and literature cited therein.

(26) Cf., e.g.: Huang, J. T. J.; Rabalais, J. W. In "Electron Spectroscopy: Theory, Techniques, and Applications"; Academic Press: London, 1978; Vol. 2, p 218.

(27) Robin, M. B.; Kuebler, N. A.; Brundle, C. R. In "Electron Spectroscopy"; North Holland Publishing Co.: Amsterdam, 1972, p 351.

(28) Brundle, C. R.; Robin, M. B.; Basch, H. *J. Chem. Phys.* 1970, 53, 2196.

(29) Bieri, G.; Asbrink, L.; Niessen, W. v. *J. Electron Spectrosc. Relat. Phenom.* 1981, 23, 281.

(30) Asbrink, L.; Niessen, W. v.; Bieri, G. *J. Electron Spectrosc. Relat. Phenom.* 1980, 21, 93.

(31) Brundle, C. R.; Robin, M. B.; Kuebler, N. A.; Basch, H. *J. M. Chem. Soc.* 1972, 94, 1451, 1466.

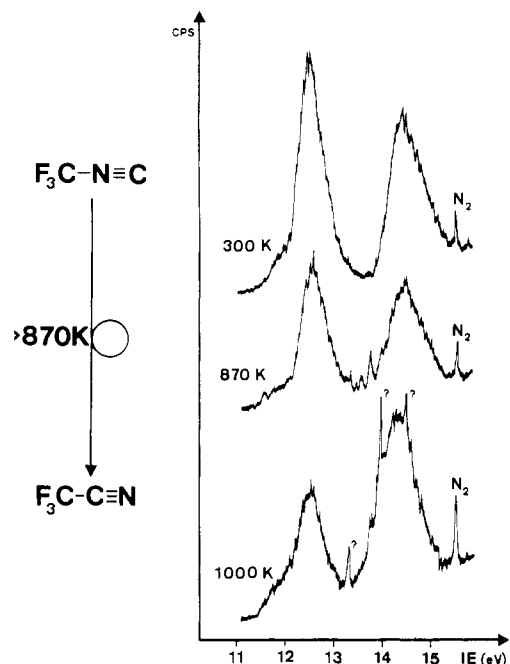


**Figure 4.** He I PE spectra for the thermal rearrangement of F<sub>3</sub>CNC to F<sub>3</sub>CCN (see text).

**Table III.** MNDO Total Energies, Heats of Formation, and Eigenvalues for Some Isomers of the C<sub>2</sub>F<sub>3</sub>N Ensemble

C <sub>2</sub> F <sub>3</sub> N	$-E_{\text{total}}^{\text{MNDO}}(\text{M})$ , eV	$\Delta H_f^{\text{MNDO}}(\text{M})$ , kJ/mol	$-\epsilon_1^{\text{MNDO}}$ , eV
F <sub>3</sub> CC≡N	1900.74	-475.8	14.80 (14.3) <sup>a</sup>
F <sub>3</sub> CN≡C	1899.75	-380.3	13.58 (12.6) <sup>a</sup>
F <sub>2</sub> C≡N=CF	1898.32	-242.3	12.06
F <sub>2</sub> C=C=NF	1897.88	-200.1	11.05
F <sub>2</sub> C=N=CF <sub>2</sub>	1897.80	-191.9	9.58
F <sub>2</sub> C=C(F)N <sup>b</sup>	1897.39	-152.1	10.08
FC≡N=CF	1896.15	-7.8	10.87
FC≡CNF <sub>2</sub>	1895.05	+17.6	11.58

<sup>a</sup> Experimental IE<sub>1</sub><sup>v</sup>. <sup>b</sup> Singlet.

### Thermal Rearrangement of F<sub>3</sub>CNC to F<sub>3</sub>CCN and Relative Stabilities of the Isomers C<sub>2</sub>F<sub>3</sub>N and C<sub>2</sub>H<sub>3</sub>N

The quantum chemically predicted<sup>2,6</sup> thermal rearrangement of trifluoromethyl isocyanide to trifluoroacetonitrile (2) can be visualized in a PE spectroscopically monitored flow system.<sup>3</sup> The following changes in the ionization patterns are observed with increasing temperature (Figure 4): The intensity of the isocyanide 12.6-eV band decreases, while the second band around 14.5 eV increases simultaneously due to the overlap with the first band of the newly formed isomer F<sub>3</sub>CCN (Figures 1, 2, and 4). Judged from the band intensities, the conversion starts at about 750 K and is about 50% complete at 1000 K. The remarkable stability of F<sub>3</sub>CNC in the gas phase in vacuo contrasts sharply with the rapid conversion in bulk even at temperatures below 200 K, experimentally supporting the calculated barrier for an unimolecular rearrangement of about 300 kJ/mol.<sup>2,6</sup>

Additional information for the preparative fluorine chemist, as to which other C<sub>2</sub>F<sub>3</sub>N isomers might be sufficiently stable to allow synthesis and characterization, can be obtained from the calculations. For this purpose, the thermodynamic stabilities of some C<sub>2</sub>F<sub>3</sub>N compounds are displayed in Figure 5; the  $\Delta\Delta H_f^{\text{MNDO}}$  values listed also in Table III denote the differences between the heat of formation  $\Delta H_f^{\text{MNDO}}$  calculated for the respective molecule and that of the most stable isomer, F<sub>3</sub>CCN. Analogous values for the parent C<sub>2</sub>H<sub>3</sub>N molecules have been added for comparison and with reference to the

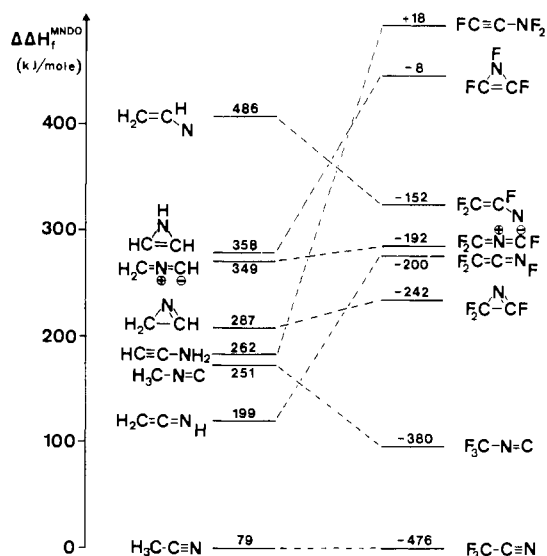


**Figure 5.** Absolute and relative MNDO heats of formation for some molecules of the C<sub>2</sub>X<sub>3</sub>N ensembles (see text).

introductory remarks on the thermal decomposition of the hazardous vinyl azide (1) in a PE spectroscopically monitored flow system,<sup>2,3</sup> which yields first 2*H*-azirine and at higher temperature acetonitrile as the most stable C<sub>2</sub>H<sub>3</sub>N isomer—an experimental observation that can be rationalized by an MNDO hypersurface study for a concerted nitrogen extrusion.<sup>4</sup>

The diagram of relative thermodynamical stabilities for the neutral molecules M (Figure 5) displays the following features: As in the case of the C<sub>2</sub>H<sub>3</sub>N ensemble, trifluoroacetonitrile is the most stable C<sub>2</sub>F<sub>3</sub>N isomer. Trifluoromethyl isocyanide, however, comes in a surprisingly close second, with a cyanide-isocyanide splitting of only 96 kJ/mol as opposed to 172 kJ/mol for the parent compounds.<sup>2,3,20</sup> Of the remaining isomers, those without NF bonds exhibit a slight increase in their relative stabilities whereas those with NF bonds are strongly destabilized; in the case of trifluoroacetylene amine by as much as 366 kJ/mol. The next isomer within the C<sub>2</sub>F<sub>3</sub>N stability sequence, 2,2,3-trifluoro(2*H*)azirine, in spite of its tendency to rearrange to F<sub>3</sub>CCN, may well be worth some synthetic effort; the parent compound, 2*H*-azirine, can be isolated.<sup>2,3,20,32</sup>

From the MNDO calculations, also a rough estimate on the stability of the corresponding radical cations, C<sub>2</sub>H<sub>3</sub>N<sup>+</sup> and C<sub>2</sub>F<sub>3</sub>N<sup>+</sup>, in their doublet states can be achieved, which may be of interest to mass spectroscopists: in a simplified approach, the calculated MNDO eigenvalue, i.e. via Koopmans' theorem,  $-\epsilon_j^{\text{MNDO}} = \text{IE}_j^{\text{v}}$ , an approximation of the vertical first ionization energy, is added to the MNDO total energy of the neutral molecule. Several surprising changes take place in comparing the stabilities of neutral molecules and their radical cations: thus F<sub>2</sub>C=N=CF<sup>+</sup> and H<sub>2</sub>C=C=NH<sup>+</sup><sup>3,33</sup> are now predicted to be the most stable species. In general, the differences in ionization energies far outweigh any but the most drastic differences in the ground-state energies. One of the energetically more favorable contenders, the perfluoro(2*H*)azirine radical cation, should spontaneously rearrange to perfluorovinylnitrene without an appreciable barrier. For F<sub>3</sub>C-CN<sup>+</sup> and F<sub>3</sub>CNC<sup>+</sup> a reversal in radical cation stabilities

(32) Guillemin, J. C.; Denis, J. M.; Lasue, M. C.; Ripoll, J. L. *J. Chem. Soc., Chem. Commun.* **1983**, 238.

(33) A more rigorous treatment of the C<sub>2</sub>X<sub>3</sub>N<sup>+</sup> radical cations by fully geometry-optimized MNDO calculations leaves the C<sub>2</sub>F<sub>3</sub>N<sup>+</sup> isomer sequence unchanged. Within the C<sub>2</sub>H<sub>3</sub>N<sup>+</sup> ensemble, however, some changes take place: the most notable one concerns the energy gain for H<sub>2</sub>C=C=NH<sup>+</sup> on complete linearization, leading to the prediction that this isomer should be more stable than the nitrile ylide, H<sub>2</sub>C=N=CH<sup>+</sup>.

is calculated making  $F_3CNC^+$  some 25 kJ/mol more favorable. This is in accordance with the observation that the molecular peak in the mass spectrum is several times more intense for  $F_3CNC$  than for  $F_3CCN$ .<sup>34</sup>

As an additional result of the geometry-optimized  $\Delta SCF$  (MNDO) calculations, one also can obtain an approximation for the adiabatic first ionization energies, i.e. the energy difference between the ground state of the neutral molecule and that of the radical cation in their equilibrium geometries. The results, 12.5 eV for  $F_3CNC$  and 13.9 eV for  $F_3CCN$ , can be checked by the onset of the respective first PE bands (Figures 1 and 2); the satisfactory agreement again lends credence to the reliability of the employed computational

methods also for highly fluorinated compounds.

**Acknowledgment.** This project has been supported by the Land Hessen, the City of Berlin, the Deutsche Forschungsgemeinschaft, and the Fonds der Chemischen Industrie. The MNDO program has kindly been provided by M. J. S. Dewar. R.D. wishes to thank the Studienstiftung des Deutschen Volkes for a scholarship.

**Registry No.**  $H_2C=CHN$ , 64987-66-2;  $HC=CHNH$ , 157-17-5;  $H_2C=N^+=CH$ , 89554-95-0;  $H_2CCH=N$ , 157-16-4;  $HC=CNH_2$ , 52324-04-6;  $H_3CN=C$ , 593-75-9;  $H_2C=C=NH$ , 17619-22-6;  $H_3CCN$ , 75-05-8;  $FC=CNF_2$ , 89554-96-1;  $FC=CFNF$ , 89554-97-2;  $F_2C=CFN$ , 89554-98-3;  $F_2C=N^+=CF$ , 89554-99-4;  $F_2C=C=NF$ , 89555-00-0;  $F_2CFF=N$ , 89555-01-1;  $F_3CN=C$ , 19480-01-4;  $F_3CCN$ , 353-85-5.

(34) Holzmann, G.; Lentz, D., private communication.

Contribution from the Istituto Chimico dell'Università and Centro di Studio sulla Fotochimica e Reattività degli Stati Eccitati dei Composti di Coordinazione del CNR, 44100 Ferrara, Italy

## Cyano-Bridged Ruthenium(II)/Platinum(II) Complexes: Synthesis, Photophysical Properties, and Excited-State Redox Behavior

CARLO ALBERTO BIGNOZZI and FRANCO SCANDOLA\*

Received July 14, 1983

Two addition compounds between the  $Ru(bpy)_2(CN)_2$  chromophore and the  $Pt(dien)^{2+}$  moiety,  $[(CN)(bpy)_2RuCNPt(dien)]^{2+}$  and  $[(dien)PtNC[Ru(bpy)_2]CNPt(dien)]^{4+}$ , have been prepared and isolated as perchlorate salts. Spectroscopic data (IR, UV/vis, luminescence) clearly indicate that in both complexes the ruthenium and platinum metal ions are bonded via cyanide bridges. The complexes are luminescent in fluid solution, with emission wavelengths (in the 580–630-nm range) and lifetimes (in the 60–630-ns range) depending on the solvent. The half-wave redox potentials in DMF solutions have been measured and found to be always more positive than those of the parent  $Ru(bpy)_2(CN)_2$  complex. Both cyano-bridged complexes behave as powerful excited-state reductants (half-wave potentials  $-1.16$  and  $-1.45$  V vs. SCE in DMF). The excited states of both complexes are quenched by methylviologen at diffusion-controlled rates by an electron-transfer mechanism. Laser flash photolysis indicates substantial yields of cage escape for these reactions. The properties of the new bimetallic complexes are compared with those of the parent  $Ru(bpy)_2(CN)_2$  compound.

### Introduction

Metal polypyridine complexes have attracted in recent years an extraordinary deal of attention. This is partly due to the peculiar combination of redox potentials, chemical inertness, and excited-state lifetimes that makes them one of the most attractive class of sensitizers for photochemical water cleavage.<sup>1-3</sup> As a step toward the development of new photosensitizers, we are interested in studying the possibility and consequences of binding additional metallic centers to a metal polypyridine chromophore. Provided that the presence of the new metallic center does not destroy the useful redox and excited-state properties of the main chromophore, such polymetallic species could exhibit some very interesting photochemistry and thermal chemistry, particularly from the viewpoint of the competition between inter- and intramolecular electron-transfer pathways. Hopefully, suitably engineered molecules of this type could lead to highly efficient charge separation in the photochemical electron-transfer step of water-cleaving photochemical cycles. A very attractive metal polypyridine chromophore is from this point of view the dicyanobis(2,2'-bipyridine)ruthenium(II),  $Ru(bpy)_2(CN)_2$ , complex. This complex has a good combination of ground- and excited-state properties and behaves in many relevant aspects as its more famous congener tris(bipyridine)ruthenium(II),  $Ru(bpy)_3^{2+}$ . In addition, it offers two potential binding

sites for other metals at the cyanide ligands.

Binuclear complexes containing cyanide-based bridging ligands have been extensively studied. The metal-containing moieties have been more frequently  $Fe(CN)_5^{n-}$ ,<sup>4,5</sup>  $Co(NH_3)_5^{3+,5,6}$   $Co(CN)_5^{2-,7}$   $Ru(NH_3)_5^{n+,8-11}$  and  $Ru(CN)_5^{3-,6,7,12,13}$  ( $n = 2,3$ ), whereas the bridging ligands include cyanide itself,<sup>4,6-8,12,13</sup> dicyanogen,<sup>9</sup> dinitriles,<sup>10</sup> dicyanamide,<sup>11</sup> and cyanopyridines.<sup>5</sup> Very recently, Kinnaird and Whitten<sup>14</sup> have reported on the formation of adducts between  $Ru(bpy)_2(CN)_2$  and silver(I) ions while similar interactions with copper(II), nickel(II), and cobalt(III) ions had been previously invoked to explain some static quenching results.<sup>15</sup>

In a preliminary communication,<sup>16</sup> we described the formation in solution of neutral adducts between  $Ru(bpy)_2(CN)_2$  and a number of platinum(II) olefin complexes. These adducts, while exhibiting interesting photophysical properties,

(1) Balzani, V.; Bolletta, F.; Gandolfi, M. T.; Maestri, M. *Top. Curr. Chem.* **1978**, *75*, 1.  
(2) Sutin, N.; Creutz, C. *Pure Appl. Chem.* **1980**, *52*, 2717.  
(3) Kalyanasundaram, K. *Coord. Chem. Rev.* **1982**, *46*, 159.

(4) Glauser, R.; Hauser, U.; Herren, F.; Ludi, A.; Roder, P.; Schmidt, E.; Siegenthaler, H.; Wenk, F. *J. Am. Chem. Soc.* **1973**, *95*, 8457.  
(5) Szecsy, A. P.; Haim, A. *J. Chem. Soc.* **1982**, *104*, 3063.  
(6) Vogler, A.; Kunkely, H. *Ber. Bunsenges. Phys. Chem.* **1975**, *79*, 83.  
(7) Vogler, A.; Kunkely, H. *Ber. Bunsenges. Phys. Chem.* **1975**, *79*, 301.  
(8) Vogler, A.; Kisslinger, J. *J. Am. Chem. Soc.* **1982**, *104*, 2311.  
(9) Tom, G. M.; Taube, H. *J. Am. Chem. Soc.* **1975**, *97*, 5310.  
(10) Krentzien, H.; Taube, H. *Inorg. Chem.* **1982**, *21*, 4001.  
(11) Sutton, J. E.; Krentzien, H.; Taube, H. *Inorg. Chem.* **1982**, *21*, 2842.  
(12) Bagger, S. *Acta Chem. Scand. Ser. A* **1980**, *A34*, 63.  
(13) Bagger, S.; Stolze, P. *Acta Chem. Scand., Ser. A* **1981**, *A35*, 509.  
(14) Kinnaird, M. G.; Whitten, D. G. *Chem. Phys. Lett.* **1982**, *88*, 275.  
(15) Demas, J. N.; Addington, J. W.; Peterson, S. H.; Harris, E. W. *J. Phys. Chem.* **1977**, *81*, 1039.  
(16) Bartocci, C.; Bignozzi, C. A.; Scandola, F.; Rumin, R.; Courtot, P. *Inorg. Chim. Acta* **1983**, *76*, L119.